A Comprehensive Approach to Skin Cancer Detection: Mixed Dataset, Optimizer Enhancement, and Web Integration

Ahmed A. Mageed, Ayman EL-SAYED, Mohammed Abdelwahad Gaber, Talaat Abdelhamid

***Abstract*— Skin cancer is a growing global health concern, and early detection is essential for effective treatment. Deep learning algorithms show promise for skin cancer diagnosis, particularly for self-monitoring applications. However, current systems are limited by narrow training datasets and lack of real-world flexibility. This study proposes a robust deep learning framework with an enhanced optimizer to address these challenges. Experiments on the ISIC, HAM10000, and a mixed dataset demonstrate improved accuracy and generalization compared to regular optimizers. The approach emphasizes the need for better dataset diversity, model accuracy, and user experience for broader adoption. This paper aims to improve skin cancer detection by leveraging an optimized convolutional neural network model, incorporating a mixed dataset, enhanced optimizer, and web integration for early diagnosis. In this paper we introduce a mixed dataset (i.e., ISIC, DermNet, and Images collected from Egyptian hospitals). The innovation lies in the creation of a diverse dataset, a novel optimizer, and a user-friendly web application, which collectively enhance detection accuracy and accessibility. The obtained results of the enhanced optimizer using the ISIC and HAM10000 datasets, are efficient as compared with Adam optimizer. It was observed that, the best performance was achieved by applying the enhanced optimizer to the mixed dataset.**

***Keywords*— Skin Cancer - Optimizer – Deep Learning – Datasets - Early detection - Computer-aided design (CAD) systems – Dermoscopy.**

I. INTRODUCTION

Skin cancer, especially malignant melanoma, is a significant global health issue with rising incidence and high mortality rates. In 2022, there were about 330,000 new melanoma cases and nearly 60,000 deaths. The highest incidence rates are in Australia and Denmark, affecting men more than women, particularly the middle-aged and elderly. Early detection is crucial, with a 5-year relative survival rate of 94.1% in the US [1-2]. Current diagnostic methods, including visual exams and biopsies, rely on clinician expertise, leading to variable accuracy. Dermoscopy improves visualization but still depends on expert interpretation [3]. AI and ML-based CAD systems analyze large datasets to detect melanoma patterns, enhancing early detection and aiding decision-making. AI can outperform human experts in some tasks but is meant to complement them [4-5]. Integrating AI into clinical practice faces challenges like inconsistent image resolution, precise segmentation, and generalization across datasets. The computational complexity of AI algorithms also presents obstacles for real-time use, requiring careful integration and proper training for healthcare professionals [6-7]. Standardizing dataset documentation and exploring approaches like Siamese neural networks with triplet loss can improve accuracy and sensitivity [8-9]. This research aims to enhance CAD techniques for skin cancer detection by developing a diverse mixed dataset, creating a novel optimizer, and constructing a user-friendly web application. The system will undergo rigorous testing to ensure accuracy and reliability, addressing current diagnostic limitations [10-11]. Leveraging AI and ML, this research seeks to improve early detection and patient outcomes [12-13]. In 2022, over 331,722 new cases of skin cancer were reported [14]. Tables 1 and 2 list the countries with the highest skin cancer incidence and deaths, with Australia and Denmark having the highest rates. Age-standardized rates (ASR) allow for accurate comparisons across populations. Table 2 shows skin cancer deaths, in 2022, with New Zealand having the highest overall mortality rate from skin cancer, followed by Norway.

Figure 1 indicates that from 2017 to 2021 in the U.S. melanoma of the skin was most commonly diagnosed in individuals aged 65–74. This age group had the highest incidence of new melanoma cases, reflecting increased risk due to cumulative sun exposure and age-related factors. The data highlights the importance of skin cancer prevention and monitoring in older adults

Manuscript received [27 August 2024]; revised [1 January 2025]; accepted [27 January 2025]. Date of publication [28 January 2025].

The work of Talaat Abdelhamid was partially supported by the Science and Technology Development Fund (STDF) of Egypt, project No: 39385." (*Corresponding author: **Talaat Abdelhamid**).*

Ahmed A. Mageed is with the Faculty of Electronic Engineering, Menoufia University, PO Box 32952, Menouf, Egypt (e-mail: mageed_ahmed@hotmail.com).

Ayman EL-SAYED was with the Faculty of Electronic Engineering, Menoufia University, PO Box 32952, Menouf, Egypt (e-mail: ayman.elsayed@el-eng.menofia.edu.eg).

Mohammed Abdelwahad Gaber is with the Dermatology and Venereology, Faculty of Medicine, Menoufia University, Shibin El Kom, Egypt.

Talaat Abdelhamid is with the Faculty of Electronic Engineering, Menoufia University, PO Box 32952, Menouf, Egypt. (e-mail: talaat_abdelhamid@el-eng.menofia.edu.eg).

TABLE 1. SKIN CANCER RATES IN 2022 FOR 10 COUNTRIES, [14].

Rank	Country	Number	ASR/100,000
	World	331,722	3.2
1	United States of America	101,388	16.5
2	Germany	21,976	12.1
3	United Kingdom	19,712	15.3
4	Australia	16,819	37.0
5	France (metropolitan)	15,729	13.5
6	Italy	13,769	12.7
7	Russian Federation	12,903	5.3
8	Canada	11,383	14.5
9	Brazil	9,676	3.3
10	China	8,789	0.37

TABLE 2. SKIN CANCER DEATHS IN 2022 FOR 10 COUNTRIES, [14]

Rank	Country	Number	ASR/100,000
	World	58,667	0.53
1	United States of America	7,368	1.0
2	China	5,385	0.20
3	Russian Federation	3,928	1.5
4	Germany	3,303	1.4
5	United Kingdom	2,626	1.5
6	Italy	2,463	1.5
7	Brazil	2,273	0.73
8	India	2,197	0.16
9	France (metropolitan)	2,087	1.4
10	Poland	1,882	1.9

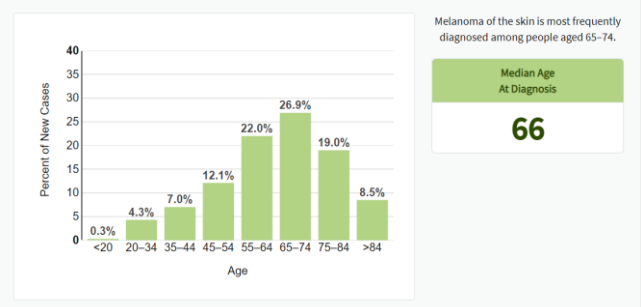

FIGURE 1 PERCENTAGE OF NEW MELANOMA SKIN CANCER CASES BY AGE GROUP IN US, [15]

Figure 2 presents data on melanoma-related deaths across different age groups in the U.S. from 2018 to 2022. The analysis highlights that the percent of deaths due to melanoma of the skin is highest among individuals aged 65–74. This trend underscores the increased risk of melanoma-related mortality in this age group compared to others.

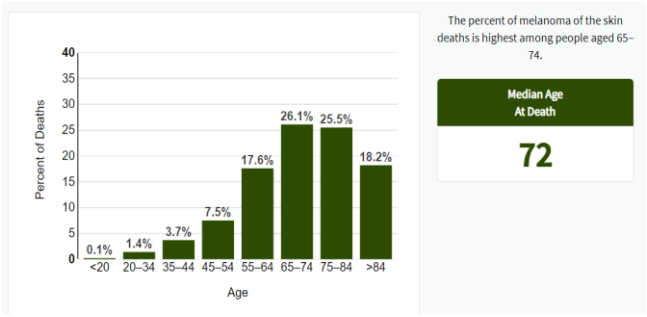

FIGURE 2 MELANOMA-RELATED MORTALITY BY AGE GROUP IN THE U.S. (2018–2022), [15].

This paper enhances skin cancer detection by developing an optimized deep learning framework that integrates diverse datasets and a web-based application for early diagnosis, featuring a mixed dataset and enhanced optimizer to overcome limitations of existing methods.

The paper is organized as follows: Section 2 introduces the related work and overview of the research in skin cancer detection. Section 3 presents the proposed methodology and introduces the mixed dataset, enhanced optimizer, and web-Based software for skin cancer detection. Section 4 introduces the results and discussions for the performance evaluation of the proposed approach. The conclusion summarizes the findings and highlights the significance of the study as presented in Section 5.

II. Related Work

Skin cancer, particularly melanoma, has garnered significant research interest due to its growing incidence and mortality risk. The ISIC (International Skin Imaging Collaboration) Archive plays a pivotal role by providing extensive dermoscopic image datasets that are critical for advancing melanoma detection through machine learning techniques. Notably, the ISIC 2018 and 2020 challenges have delivered valuable annotated datasets, which are fundamental for developing and evaluating skin cancer detection algorithms [16]. Research utilizing these datasets has led to significant advancements. The research gaps include the need for more diverse and balanced datasets to address biases in skin cancer classification. Further improvements are needed in handling less common skin cancer types and enhancing the model's robustness across various image qualities. Additionally, exploring real-time model performance in clinical settings remains a key area for future research. ISIC and HAM10000 datasets are essential for advancing melanoma detection, with ISIC providing a wide range of dermoscopic images annotated for skin cancer classification. The analysis of these datasets reveals significant trends, such as the increasing number of dataset downloads, with top datasets representing the majority of traffic. Furthermore, the integration of metadata, such as patient demographics and clinical information, has been shown to improve model performance by offering richer data for training. The incorporation of synthetic data augmentation, through methods like GANs, haTas further enhanced the diversity of images, helping to improve model robustness and accuracy.

Deep convolutional neural networks (CNNs) achieve dermatologist-level accuracy in skin cancer classification using large clinical image datasets. Ensemble learning, as shown in the ISIC 2018 challenge, enhances diagnostic accuracy by combining models [17]. Metadata and patient demographics improve melanoma classification. GANs create realistic dermoscopic images, boosting model accuracy [18]. Clear AI models increase transparency and trust in diagnostics [19]. Improved dataset documentation on Hugging Face is needed for better reproducibility and transparency [20-21]. Yang, Liang, and Zou [22] found exponential dataset growth and power-law distribution in downloads but noted gaps in documentation.

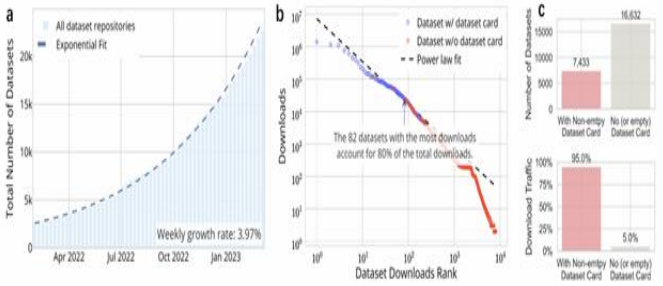

FIGURE 3 COMPREHENSIVE ANALYSIS OF 24,065 DATASETS ON HUGGING FACE, YANG ET AL, [22].

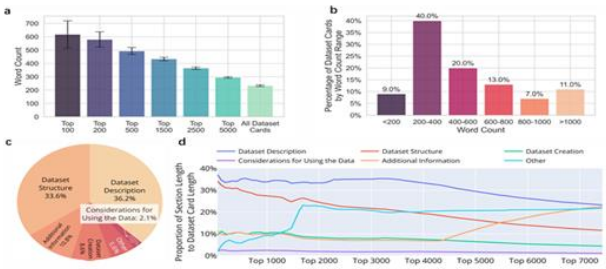

FIGURE 4. SECTION LENGTH AND POPULARITY IN DATASET DOCUMENTATION, [22].

Their analysis [22], shown in Figure 4b, reveals that 91.0% of the top 100 downloaded dataset cards are detailed, with over 200 words. The Dataset Description and Dataset Structure sections are the most comprehensive, comprising 36.2% and 33.6% of the documentation, respectively, while the section on data usage considerations is notably brief at 2.1%. Figure 4a indicates that highly downloaded datasets tend to have more extensive documentation, while less popular ones focus on the Additional Information section. This underscores the need for better documentation practices, especially for ethical considerations and usability. Deep Neural Networks (DNNs) use first-order (e.g., GD, Adam, NosAdam) and second-order optimization methods. First-order methods adjust learning rates based on gradient statistics but need tuning [23-24]. Adam improvements like Lookahead and SWATS enhance performance [25-26]. Second-order methods use the Hessian matrix for precise steps but are computationally intensive [27]. Enhanced Adam variants improve convergence and accuracy [28-29]. AAdam outperforms Adam and NAdam in reducing loss and achieving higher accuracy, despite higher memory use [32]. Ahmed et al. [33] show that Nadam, Adam, RMSProp, and Adamax achieve high accuracy, while AdaDelta, Adagrad, and SGD are less suitable for skin cancer detection.

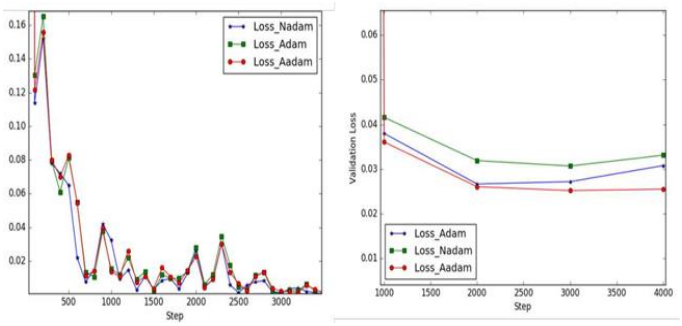

FIGURE 5. COMPARISON OF LOSS VALUE VARIATIONS: AADAM VS. ADAM AND NADAM, [32].

Figure 6 shows the loss validation curves over epochs for RMSProp, Nadam, AdaDelta, SGD, Adamax, Adagrad, Adam, and Adam-M. The first group (AdaDelta, Adagrad, SGD) has high loss validation, making them unsuitable for early skin cancer detection, while the second group [34-35] performs better with lower loss validation. Adam-M and Adam exhibit stable loss curves without overfitting. Using the HAM10000 dermoscopy dataset, deep learning and transfer learning models were developed to process images without feature extraction or preprocessing.

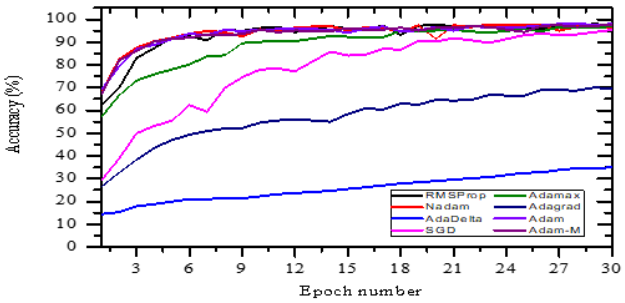

FIGURE 6. DEPENDENCE OF ACCURACY ON EPOCHS NUMBER FOR VARIOUS OPTIMIZERS, [33]

Figure 7 shows training loss curves for RMSProp, Nadam, AdaDelta, SGD, Adamax, Adagrad, Adam, and Adam-M. Early skin cancer detection with dermoscopic images aids faster, cost-effective diagnosis [32]. Nadam, Adam, Adam-M, RMSProp, and Adamax achieve high accuracy with more epochs, with customized Adam excelling in speed and accuracy. These findings underscore the importance of optimizers in deep learning for skin cancer classification. Tools like DUNEScan's Grad-CAM, SkinVision, and IBM Watson's Dermatologist AI effectively detect skin abnormalities.

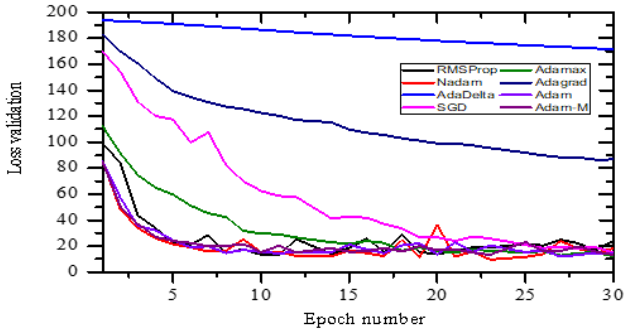

FIGURE 7. LOSS VALIDATION CURVES FOR VARIOUS OPTIMIZERS, [33]

Table 3 highlights key studies on skin cancer detection. The highest accuracy (98.7%) was achieved in [41]. Other notable works include 95% accuracy [49] and 94.7% accuracy [47-63]. For the ISIC dataset, the best accuracy was 98.7% in 2023. Other studies include 92.5% and 95.62% accuracy. For the HAM10000 dataset, the best result was 95% accuracy [10]. Other studies reported 93.1% and 89.5% accuracy. The best overall result was 98.7% on the ISIC dataset using a multi-modal approach with CNNs and a fusion attention module.

The related works show significant progress in skin cancer detection using deep learning models like CNNs and transfer learning. Models such as VGG, Inception V3, and EfficientNet have achieved high accuracies (up to 98%) on datasets like ISIC. Data augmentation and advanced optimizers, like AAdam, have further improved model performance. However, limitations exist in dataset diversity, with many studies lacking representation of various skin tones, potentially reducing generalizability. Additionally, model interpretability remains a challenge, as many deep learning models are considered 'black boxes.' Despite high accuracy, clinical validation and real-world testing are still necessary for broader deployment.

III. Proposed Methodology

In this paper, we developed a novel dataset, incorporating newly curated images to improve skin cancer detection models. We also propose an enhanced optimizer framework to achieve the high-performance metrics. The new Mixed Dataset will be systematically compared to established benchmark datasets in medical image analysis, with a comprehensive evaluation of its efficacy. Our methodology includes refining an Enhanced Optimizer, rigorously tested on both the Mixed Dataset and other widely adopted optimizers to assess its generalization. A comparative analysis will identify the most effective optimizer-dataset combinations, based on accuracy, sensitivity, specificity, and computational efficiency. Finally, the selected optimizer and dataset will be integrated into a web-based application for clinical use, aiming to improve skin cancer detection and advance medical image analysis.

3.1 Mixed Dataset

The need for new skin cancer datasets is significant due to the limitations of existing datasets, which often lack demographic diversity and are relatively small in size. This can hinder the adaptability of diagnostic models across different ethnicities and skin types. New datasets with broader demographics and larger image collections are essential for developing inclusive and accurate diagnostic tools.

Technological advancements in imaging and the inclusion of comprehensive metadata, such as patient history and lesion progression, further underscore the need for updated datasets. To address these gaps, we created the "Mixed Dataset" combining skin cancer images sourced from Egyptian hospitals, with approval from the Egyptian Ministry of Health, and integrating them with images from the ISIC and DermNet datasets. This new dataset aims to enhance research, improve diagnostic precision, and ultimately advance dermatological practice.

ISIC and DermNet datasets have limitations affecting skin cancer detection models. ISIC has class imbalance, poor image quality, inconsistent annotations, and limited darker skin tone representation, leading to biased training. DermNet is smaller, with similar quality issues and limited demographic diversity. Both lack comprehensive clinical context, reducing model reliability. Updating these datasets with balanced classes, diverse skin tones, and consistent annotations is crucial for better performance and fairness.The creation of the Mixed Dataset addresses the limitations of existing datasets like ISIC and HAM10000, which lack demographic diversity and have class imbalances. While ISIC and DermNet provide 2357 and 4382 images respectively, they primarily represent specific populations, limiting model effectiveness across diverse skin types. To improve this, the Mixed Dataset includes 1443 images from Egyptian hospitals, bringing the total to 8062 images and enhancing representation for crucial classes, such as melanoma. By adding more diverse samples and including metadata like patient histories, the Mixed Dataset aims to train more inclusive, effective models for skin cancer detection, better suited for real-world clinical use. Table 4 details the number of photos for various skin lesion categories across ISIC, DermNet, and the Mixed Dataset. We collaborated with the Egyptian Ministry of Health to collect and photograph cases, adhering to ethical standards and patient privacy. These images were integrated with public datasets to enhance the diversity and accuracy of the Mixed Dataset, providing a valuable resource for improving skin cancer detection and diagnosis.

Table 3. Summary of Skin Cancer Research Studies.

Year	Name	Objective	Techniques	Dataset	Detection Accuracy	Classification Accuracy	References
2024	Skin Cancer Segmentation and Classification Using Vision Transformer	Create a Vision Transformer model specifically designed for the purpose of segmenting and classifying skin cancer.	Vision Transformer, deep learning	ISIC 2020, HAM10000	N/A	92.5%	[36]
2024	Leveraging Knowledge Distillation for Lightweight Skin Cancer Classification	Balance accuracy and computational efficiency in skin cancer classification	Knowledge distillation, machine learning	ISIC 2020	N/A	90.2%	[37]
2024	Skin Cancer Recognition Using Unified Deep Convolutional Neural Networks	Performance comparison of YOLO-based models for skin lesion classification	YOLOv3, YOLOv4, YOLOv5, YOLOv7	ISIC 2020	N/A	86.3%	[38]
2024	Skin Cancer Detection and Classification Using Neural Network Algorithms	Assess efficacy of neural network algorithms for skin cancer detection	Neural network algorithms	ISIC, HAM10000	٩١.٢٠%	٩١.٢٠%	[39]
2023	Artificial Intelligence for Skin Cancer Detection	To categorize and classify the various AI-based technologies employed for the detection and categorization of skin cancer.	Convolutional Neural Networks	ISIC 2018	92.3%	N/A	[40]
2023	Joint-Individual Fusion Structure with Fusion Attention Module for Multi-Modal Skin Cancer Classification	Develop a multi-modal skin cancer classification method	CNN, fusion attention module	ISIC 2020, HAM10000	N/A	98.7%	[41]
2023	Application of Machine Learning in Melanoma Detection and the Identification of 'Ugly Duckling' and Suspicious Naevi: A Review	Review machine learning applications in melanoma detection	Machine Learning	ISIC 2020	93.5%	N/A	[42]
2023	Domain Shifts in Dermoscopic Skin Cancer Datasets: Evaluation of Essential Limitations for Clinical Translation	Evaluate limitations of CNNs for clinical translation in skin cancer classification	CNN, domain shifts evaluation	ISIC, PH2	N/A	89.7%	[43]
2023	Multi-class Skin Cancer Classification Architecture Based on Deep Convolutional Neural Network	Develop and compare stacking models for skin cancer classification	Deep CNN, stacking models	ISIC 2018	N/A	87.9%	[44]
2023	CIFF-Net: Contextual Image Feature Fusion for Melanoma Diagnosis	Improve melanoma diagnosis by integrating contextual information	CIFF-Net, deep neural network	ISIC 2019	N/A	88.6%	[45]
2023	Skin Cancer Detection Using Deep Learning Approach	Review of skin cancer classification using deep learning methods	Convolutional Neural Networks	ISIC, HAM10000	95.62%	N/A	[46]
2022	Advanced Skin Cancer Detection Using Deep Learning	Integration of FrCN and residual convolutional networks for skin lesion segmentation and classification	FrCN, residual networks.	ISIC 2018, HAM10000	٩٤,٧%	N/A	[47]
2022	A Comparative Analysis of Models with VGG-16, VGG-19, and Inception V3	Comparison of VGG-16, VGG-19, and Inception V3 models for skin lesion classification	CNN models (VGG-16, VGG-19, Inception V3)	ISIC 2019	N/A	٩٢,٧%	[48]

2022	Detection of Skin Cancer using Artificial Intelligence & Machine Learning Concepts	Use of CNNs and transfer learning for skin cancer detection	CNNs, transfer learning	ISIC 2018	٩٥%	N/A	[49]
2022	Melanoma Mirage: Unmasking Skin Cancer with Deep Learning	Automated skin cancer detection using CNNs	CNNs	ISIC 2020	٩٣,٧٠%	N/A	[50]
2022	Skin Lesions Detection via Convolutional Neural Networks	Classification of melanoma from benign pigmented skin lesions using CNNs	CNNs	ISIC 2020	N/A	٨٩,٥%	[51]
2022	Enhanced Skin Cancer Classification using Deep Learning and Nature-based Feature Optimization	Combine deep learning and nature-based optimization for skin cancer classification	CNN, fuzzy k-means clustering	ISIC 2020	N/A	93.1%	[52]
2022	Detection of Skin Cancer Based on Skin Lesion Images Using Deep Learning	Detect skin cancer using deep learning on lesion images	Deep Learning	ISIC 2020	90.5%	N/A	[53]
2022	Deep Learning Methods for Accurate Skin Cancer Recognition and Mobile Application	Develop mobile application for skin cancer recognition using deep learning	Deep Learning	ISIC 2018	N/A	89.3%	[54]
2022	Classification of Skin Cancer Empowered with Convolutional Neural Network	Classify skin cancer using CNNs	CNN	ISIC 2020	N/A	N/A	[55]
2022	Skin Lesions Classification into Eight Classes for ISIC 2019 Using Deep Convolutional Neural Network and Transfer Learning	Classify skin lesions into eight classes using CNN and transfer learning	CNN, Transfer Learning	ISIC 2019	N/A	N/A	[56]
2022	Analysis and Classification of Skin Cancer Based on Deep Learning Approach	Use deep learning to analyze and classify skin cancer	Deep Learning	ISIC 2020	N/A	N/A	[57]
2022	Deep Convolutional Neural Network (DCNN) for Skin Cancer Classification	Use DCNN for early detection of skin cancer	DCNN	ISIC 2018	N/A	N/A	[58]
2022	Enhanced Skin Cancer Classification using Efficient Net B0-B7 through a Tailored Preprocessing Pipeline	Improve classification using EfficientNet B0-B7 and preprocessing	EfficientNet B0-B7, CNN	ISIC 2020	N/A	N/A	[59]
2022	Skin Cancer Detection and Classification Using Deep Learning	Develop deep learning models for skin cancer detection and classification	Deep Learning	ISIC, HAM10000	91.5%	91.5%	[60]
2022	Double AMIS-ensemble deep learning for skin cancer classification	Develop a self-use classification system using a double-AMIS ensemble model	Double-AMIS ensemble, deep learning	ISIC 2019	N/A	90.9%	[61]
2022	Skin Cancer Detection and Classification Using Neural Network	Use neural networks for skin cancer detection and classification	Neural networks	ISIC 2020	89.0%	89.0%	[62]

Figure 8 presents one sample image per class from the ISIC dataset, illustrating the visual diversity across skin lesion types. This overview helps demonstrate the unique features the model needs to recognize for effective classification.

FIGURE 8. IMAGES FROM ISIC DATASET.

FIGURE 9. IMAGES FROM MIXED DATASET.

Table 4. The MIXED Dataset.

Class Name	ISIC	Dermnet	From Egyptian hospitals DS	SUM
actinic keratosis	130	1149	211	1490
basal cell carcinoma	392	29	15	436
Dermatofibroma	111	103	18	196
Melanoma	454	463	417	1334
Nevus	373	101	422	896
pigmented benign keratosis	478	576	6	1060
seborrheic keratosis	80	1371	246	1697
squamous cell carcinoma	197	108	66	371
vascular lesion	142	482	42	582
Total	2357	4382	1443	8062

Figure 9 shows a diverse range of skin lesions from the Mixed dataset, integrating images from multiple sources for robust training. This dataset, used with HAM10000 and ISIC, assesses optimizer performance.

Images are resized, normalized, and stratified to ensure a balanced, standardized dataset for effective model training and accurate predictions.

Table 5 shows the study involves running two optimizers with three datasets. The table aims to inform the reader about the mechanism of comparing the performance of these optimizers across the datasets, helping to highlight the differences in results for each optimizer when applied to different datasets.

TABLE 5. OPTIMIZERS TESTED ON VARIOUS SKIN CANCER DATASETS

#	Dataset	Optimizer
1	HAM10000	Adam
2	HAM10000	Enhanced Optimizer
3	ISIC	Adam
4	ISIC	Enhanced Optimizer
5	Mixed Dataset	Adam
6	Mixed Dataset	Enhanced Optimizer

Figure 10 shows the imbalance in a mixed dataset after splitting it into 70% training and 30% validation. This imbalance can negatively impact model performance. To address this, data augmentation was applied to increase samples in

underrepresented classes, improving generalization. The training dataset initially had 5,640 images unevenly distributed across nine skin condition classes, with Seborrheic Keratosis being the largest class (21.046%) and Dermatofibroma the smallest (2.429%). Augmentation balanced the dataset, enhancing the model's performance across all classes.

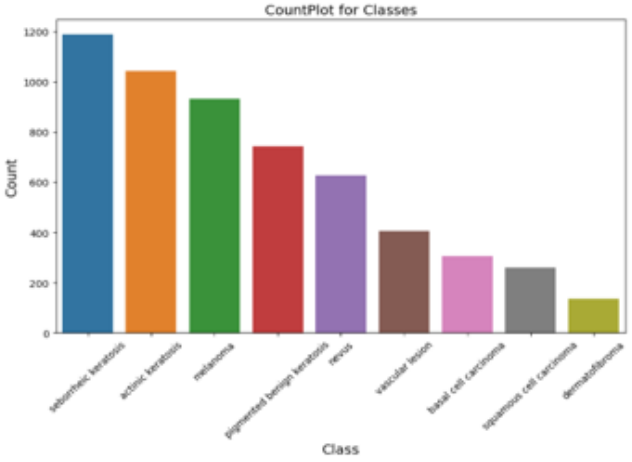

FIGURE 10. VISUALIZATION OF CLASS IMBALANCE IN MIXED DATASETS AFTER TRAINING-VALIDATION SPLIT.

Figure 11 shows that image augmentation was used to address class imbalance in the training dataset. The Augmentor library expanded the dataset to ensure equal representation of each class, essential for developing a robust skin cancer detection model [65]. The model's performance was assessed using the ISIC, HAM10000, and Mixed datasets with Adam and a custom-enhanced optimizer. The CNN, designed to classify nine skin conditions, featured five convolutional layers (32, 64, 128, 256, 512 filters), ReLU activation, MaxPooling, and dropout layers (15-25%). A dense layer with 1024 units and a softmax output layer completed the model. Using Adam with a 0.001 learning rate, the model's validation accuracy improved from 60.43% to over 97% by the 32nd epoch, demonstrating its effectiveness.

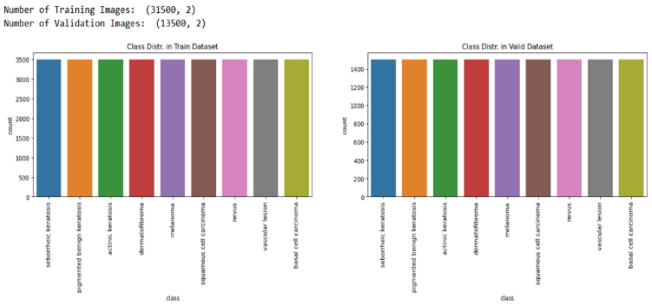

FIGURE 11. CLASS DISTRIBUTION BALANCE MIXED DATASETS AFTER DATA AUGMENTATION.

Our CNN for skin cancer classification uses five convolutional layers (32, 64, 128, 256, 512 filters) with ReLU activation and MaxPooling. Dropout layers (15-25%) prevent overfitting. The final dense layer (1024 units) and softmax activation support multi-class classification. Using the Adam optimizer (learning rate 0.001), the model achieved over 97% validation accuracy by the 32nd epoch. Each parameter was validated to enhance suitability for skin cancer detection.

3.2. A Comparison of Model Performance Using Adam and Enhanced Optimizers

On the other hand, the model using enhanced optimizer which is a custom implementation designed to offer enhanced performance and fine-tuning capabilities. It is initialized with parameters including a learning rate of 1×10^{-3}, beta values of 0.9 and 0.999, epsilon for numerical stability at 1×10^{-8}, and an option for AMSGrad. The optimizer creates slot variables for each trainable model parameter to track the first and second moments of the gradients and optionally the maximum of the second moments if AMSGrad is used. The gradient updates are applied using Tensor Flow's operation, which ensures efficient and accurate weight adjustments. During training with the enhanced optimizer, the model initially had a training accuracy of 41.60% and validation accuracy of 61.03%, indicating underfitting. By epoch 5, the accuracy improved to 91.12% on training data and 91.79% on validation data. By epoch 10, training accuracy reached 97.66% and validation accuracy 96.37%, showing strong generalization. From epochs 11 to 20, the model peaked at 98.85% training accuracy and 97.36% validation accuracy. Despite some fluctuation in validation loss between epochs 21 and 30, validation accuracy remained high, peaking at 97.50%. The enhanced optimizer effectively optimized the model, maintaining high accuracy and low loss, with early stopping helping to manage overfitting. The weight update rule with weight decay is given by:

$$w_{t+1} = w_t - \eta \cdot \left(\frac{\partial L}{\partial w_t} + \lambda\, w_t\right) \qquad (1)$$

Where w_t is the weight at time step t and η is the learning rate. The gradient of the loss function with respect to the weight is represented by $\frac{\partial L}{\partial w_t}$, λ represents the weight decay coefficient. The $\lambda\, w_t$ added by the weight decay to shrink the weights. In the custom optimizer, weight decay is incorporated as a regularization mechanism to enhance model generalization and prevent overfitting. Weight decay, also known as L_2 - regularization, penalizes large weights by adding a term proportional to the squared magnitude of the weights to the loss function. Adam is renowned for its robustness, effectiveness in handling various gradient scales, and momentum-like behavior, which expedites convergence. It can be calculated by the exponential moving average of the gradient. Let m be the first moment vector which keeps a moving average of the gradients. Let v be the second moment vector, which keeps a moving average of the squared gradients. Let β_1 and β_2 are smoothing parameters used to control the decay rates of the moving averages. Typical values are β_1 = 0.9 and β_2 = 0.999. Update the moving averages of the gradients in equations (2) and (3):

$$m = \beta_1\, m + (1 - \beta_1) * \mathrm{g} \qquad (2)$$
$$v = \beta_2\, v + (1 - \beta_2)\, \mathrm{g}^2, \qquad (3)$$

Bais – corrected moment estimates.

$$\bar{m} = m/(1 - \beta_1^t) \text{ and } \bar{v} = \frac{v}{1-\beta_2^t}, \quad (4)$$

Update the model parameters in equation (5):

$$\theta_{t+1} = \theta_t - \alpha\, \frac{\bar{m}}{\sqrt{\bar{v}} + \varepsilon}, \quad (5)$$

Where, θ_t represents the model parameters at time step t and θ_{t+1} represents the updated model parameters at time step t +1 of equation (5). This equation calculates the exponential moving average of the gradients. It maintains a record of the average gradient values throughout the training process. Adam's main advantage lies in its ability to dynamically modify the learning rate for each parameter by incorporating both first and second-moment estimates. This feature enables the Adam algorithm to effectively handle sparse gradients, noisy data, and parameters with varying scales. In the enhanced custom optimizer, the AMSGrad variant is incorporated to enhance the stability of the optimization process by addressing potential issues with the standard Adam optimizer. AMSGrad modifies

Adam's approach by maintaining a maximum of past squared gradients. AMSGrad is enabled by setting the AMSGrad parameter to True. The optimizer then uses the vhat variable to keep track of the maximum squared gradients and updates the weights accordingly. This adjustment helps to ensure more stable and reliable convergence compared to the original Adam optimizer. The enhancements in MyAdamOptimizer2 include the combination of weight decay and AMSGrad, which provides a more robust training process. Weight decay helps prevent overfitting by penalizing large weights, while AMSGrad ensures that the learning rate for each parameter remains stable, avoiding potential issues with convergence. Together, these modifications are likely to lead to better generalization and improved performance of the model across various datasets and tasks. We selected the standard Adam optimizer and an Enhanced Adam optimizer for our methodology. Adam is a top choice in deep learning due to its adaptive learning rate, which tailors individual learning rates for each parameter using first and second moments of gradients. With empirically validated hyperparameters (β_1 = 0.9, β_2 = 0.999, and learning rate 0.001), Adam provides stability and efficiency, especially in noisy or complex tasks like skin cancer detection. However, to address Adam's limitations with noisy gradients, we developed the Enhanced Adam Optimizer. A small constant ($\varepsilon = 1\times10^{-8}$) ensures numerical stability during training, preventing issues with small or noisy gradients. A dropout rate of 15-25% prevents overfitting by randomly setting a fraction of the input units to zero during training, encouraging redundant representations. A batch size of 50 ensures stable gradient updates and balances memory efficiency, affecting both training stability and the final accuracy of the model. This version dynamically adjusts the learning rate based on gradient variance, allowing for aggressive updates with consistent gradients and smaller updates when gradients are noisy. By combining these optimizers, we leverage Adam's stability while refining performance through our enhancements, aiming for better accuracy and more stable training in skin cancer detection. Using the mixed dataset, we compared the Adam and enhanced optimizers for training a skin cancer detection model. Adam achieved 98.63% final accuracy and 97.26% validation accuracy. The enhanced optimizer reached 99.23% final accuracy and 97.50% validation accuracy, showing slightly better performance. This suggests the enhanced optimizer is more effective for this model and dataset. Testing accuracy is crucial for assessing real-world performance, distinct from training and validation. We updated our model to include a test evaluation phase, achieving 98.1% testing accuracy with the enhanced optimizer on HAM10000 (see Figure 12). A graph of test accuracy and loss highlights the model's ability to generalize, addressing overfitting concerns and confirming robustness.

Figure 12 shows the performance metrics of the proposed model using an enhanced optimizer on a mixed dataset. The dataset includes nine classes, such as Actinic Keratosis, Basal Cell Carcinoma, and Melanoma, with each class evaluated based on Precision, Recall, and F1-Score. The model demonstrates strong performance, with high precision and recall values, particularly for Vascular Lesion and Squamous Cell Carcinoma, where precision reaches a perfect score of 1.00. The F1-Score consistently remains above 0.95, indicating a good balance between precision and recall. Summary metrics like Accuracy, Macro Avg, and Weighted Avg reflect an overall high model performance, achieving close to 98% accuracy. The weighted averages account for the class distribution, showing that the optimizer performs well across both major and minor classes. This highlights the optimizer's effectiveness in handling complex, real-world medical image data.

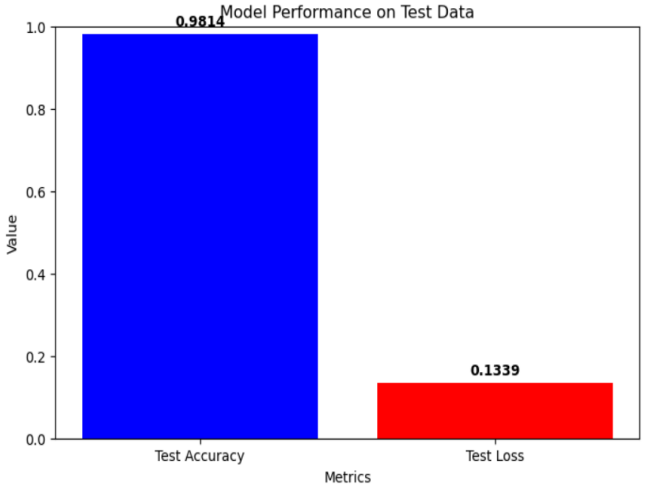

FIGURE 11. MODEL PERFORMANCE ON TEST DATA FOR ENHANCED OPTIMIZER ON HAM 10000 DATASET

We used an early stopping callback to prevent overfitting, halting training if validation loss stagnates for 10 epochs. With our enhanced optimizer on the mixed dataset, training and validation accuracies improved from 41.60% and 61.03% at epoch 1 to 98.85% and 97.36% by epoch 20. After early stopping, testing accuracy reached 98.93%, demonstrating the model's robustness and generalization ability.

3.3. Web-Based Software for Skin Cancer Detection

Our web-based software for skin cancer detection is designed to offer a user-friendly and efficient solution for diagnosing skin cancer as in presented via URL " http://197.165.160.43:100/ ". It caters to both patients and clinical organizations, enabling them to easily scan and analyze images for potential skin cancer indications. The interface is intuitive, allowing users to navigate through the software without requiring extensive technical knowledge. A key feature of this software is its flexibility in integrating with various skin cancer detection models. It supports any model provided in the H5 file format, making it compatible with a range of detection algorithms. Among the models tested, our custom-enhanced optimizer developed specifically for this purpose demonstrated superior performance when applied to a mixed dataset. The results were encapsulated in an H5 file, which was then incorporated into our software. The integration of this optimized model into the software, alongside our dedicated Application Programming Interface (API), allowed for comprehensive comparative analysis and validation. This process confirmed the enhanced optimizer's capability to deliver highly accurate detection results. By leveraging our advanced model and technology, the software not only ensures

high reliability in skin cancer detection, but also offers a robust adaptable tool for effective diagnostic support. Our web-based software uses encryption, access controls, and audits to protect patient data. Users log in with a username and password to scan skin images for cancer detection. Physicians can review and compare the model's results with their own assessments, enhancing accuracy. User interaction logs ensure data integrity and security. Figure 13 demonstrates this feature.

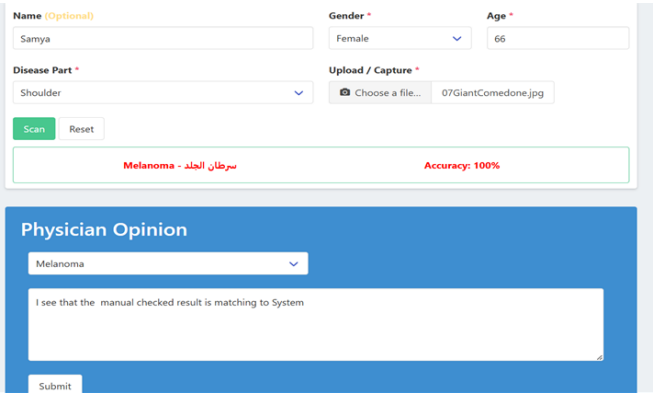

FIGURE 13. WEB SYSTEM ANALYSIS AND RESULTS COMPARISON WITH PHYSICIAN INPUTS.

Figure 14 shows the web-based skin cancer detection system architecture. It features an SQL Server database, an MS .NET interface for user interaction, and a Python API connecting to the Python model for analysis. Users upload images via the .NET interface, which are processed by the Python model, returning accurate detection results and recommendations.

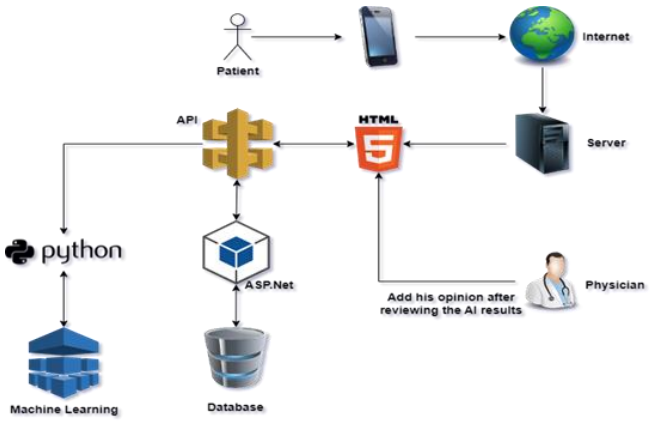

FIGURE 14. WEB BASED SKIN CANCER DETECTOR WEB BASED SYSTEM ARCITETURE.

Figure 15 illustrates the integration of a deep learning system with Electronic Health Records (EHRs), enhancing clinical workflows and patient care. This system ensures GDPR and HIPAA compliance through encryption, access controls, and audits. It undergoes rigorous validation and real-world trials to assess its diagnostic accuracy and clinical effectiveness. Comprehensive training and support are provided for healthcare professionals, along with patient educational resources. The system distinguishes between end users and admin users and is supported by a relational database managing the skin cancer detection process. Key tables include classifications, body parts, entities, scan methods, models, scans, and user accounts. We have implemented multiple security measures to safeguard patient data. Database encryption using Advanced Encryption Standard (AES) protects sensitive data at rest. An audit mechanism tracks all transactions, with changes preserved in audit tables to ensure data integrity. Additionally, a role-based access control system restricts user access according to their roles, preventing unauthorized access to sensitive information. Together, these measures enhance the application's security and protect patient confidentiality.

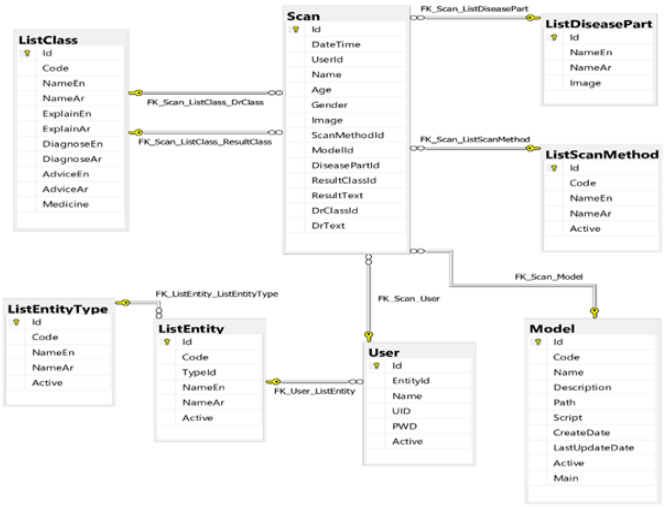

FIGURE 15. SKIN CANCER DETECTOR WEB BASED SYSTEM ENTITY-RELATIONSHIP DIAGRAM (ERD).

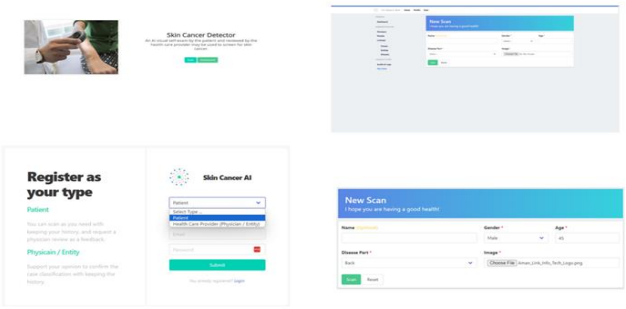

FIGURE 16. SKIN CANCER DETECTOR WEB BASED SYSTEM INTERFACE.

IV. RESULTS AND DISCUSSIONS

The creation of a new skin cancer dataset that incorporates both existing data and new images from Egyptian hospitals marks a significant contribution to the global fight against skin cancer. By integrating local data into the dataset, the mixed dataset improves its diversity to handle diverse demographics, resulting in enhanced accuracy and relevance of machine learning models for early cancer detection. This dataset not only bolsters

Egypt's scientific standing, but also provides valuable resources for researchers and medical professionals worldwide. It enables the development of more effective diagnostic tools, particularly for populations with similar demographic and environmental factors. Ultimately, this work contributes to better patient outcomes and advances the global effort to combat skin cancer. The experiments were conducted using a high-performance computing platform with an NVIDIA GPU. Python 3.8, TensorFlow 2.7, and Keras 2.7 were used for model development, with additional libraries like NumPy and Matplotlib for data handling and visualization. Key components include data preprocessing (augmentation, resizing, and normalization), CNN architecture, and training scripts. Adam and an enhanced optimizer were used, and models were saved in .h5 format for evaluation and future use.

We tested six models using Adam and an enhanced optimizer across three datasets: HAM10000, ISIC, and Mixed. By comparing accuracy and loss for each combination, we aim to identify the most effective ptimizer for each dataset, ensuring optimal results in skin cancer detection. Figure 17 compares the Adam and enhanced optimizers on the HAM10000 dataset. Figure 17(a) and 17(b) show Adam's performance with 97.90% accuracy and 0.219 loss. Figure 17(c) and 17(d) highlight the enhanced optimizer's superior performance, achieving 97.95% accuracy and 0.165 loss. These results indicate the enhanced optimizer is more effective, providing higher accuracy and reliability for skin cancer classification.

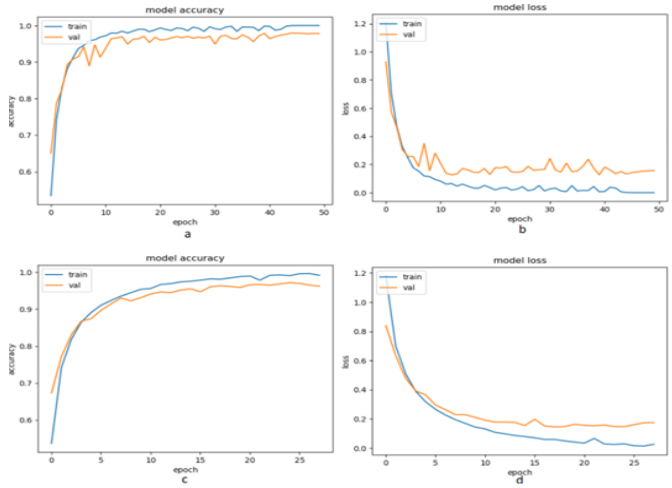

FIGURE 17. PERFORMANCE COMPARISON ON HAM10000 DATASET: ADAM VS. ENHANCED OPTIMIZER (ACCURACY AND LOSS).

Figure 18 compares Adam and enhanced optimizers on the ISIC dataset. Adam achieves 93.96% accuracy and 0.218 loss (Parts a and b). The enhanced optimizer shows 92.48% accuracy and 0.249 loss (Parts c and d), indicating Adam performs better on this dataset. This suggests Adam is more suitable for the ISIC dataset, unlike the HAM10000 dataset where the enhanced optimizer excels.

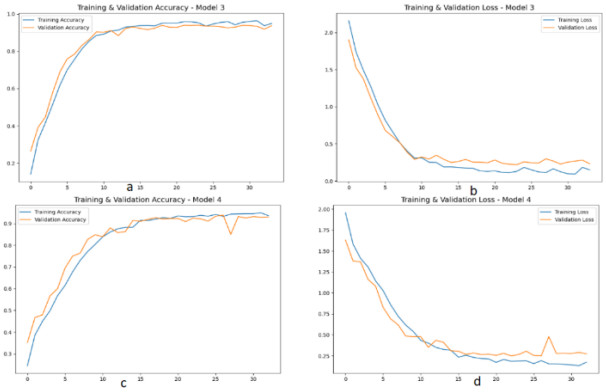

FIGURE 18. PERFORMANCE COMPARISON ON ISIC DATASET: ADAM VS. ENHANCED OPTIMIZER (ACCURACY AND LOSS).

Figure 19. compares Adam and enhanced optimizers on the Mixed Dataset, with Part (a) showing Adam's accuracy at 97.02% and Part (b) its loss at 0.096. The enhanced optimizer, shown in Parts (c) and (d), achieves 98.93% accuracy and a much lower loss of 0.032, highlighting a notable improvement over Adam.

Table 6. Adam and Enhanced Optimizer Performance Comparison Across HAM10000, ISIC, and Mixed Datasets

These results indicate that the enhanced optimizer offers superior accuracy and reliability for the Mixed Dataset.

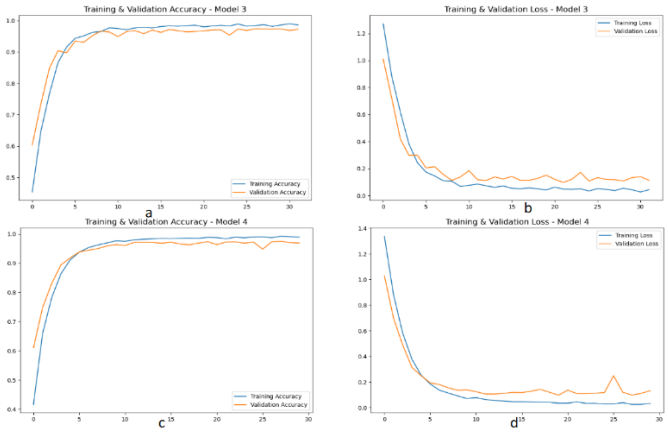

FIGURE 19. PERFORMANCE COMPARISON ON MIXED DATASET: ADAM VS. ENHANCED OPTIMIZER (ACCURACY AND LOSS).

Table 6 compares the Adam and enhanced optimizers across three datasets: HAM10000, ISIC, and Mixed. The enhanced optimizer achieves higher accuracy and lower loss on the HAM10000 (97.95%, 0.165) and Mixed datasets (98.93%, 0.032). Adam performs better on the ISIC dataset with 93.96% accuracy and 0.218 loss. Overall, the enhanced optimizer generally outperforms Adam, except on the ISIC dataset. The

proposed enhanced algorithm's training time with the mixed dataset was evaluated, with the first epoch taking 945 seconds and subsequent epochs
averaging 530–685 seconds. Total training time for 34 epochs was approximately 8 hours and 47 minutes.

TABLE 6. ADAM AND ENHANCED OPTIMIZER PERFORMANCE COMPARISON ACROSS HAM10000, ISIC, AND MIXED DATASETS

Optimizer Type	Dataset	Accuracy	Loss	Figure
Adam	HAM10000	97.90%	0.219	17 (a,b)
enhanced optimizer	HAM10000	97.95%	0.165	17 (c,d)
Adam	ISIC	93.96%	0.218	18 (a,b)
enhanced optimizer	ISIC	92.48%	0.249	18 (c,d)
Adam	Mixed Dataset	97.02%	0.096	19 (a,b)
enhanced optimizer	Mixed Dataset	98.93%	0.032	19 (c,d)

In summary, using HAM10000 dataset, our model achieves 97.90% accuracy with Adam and 97.95% with the enhanced optimizer in comparison with [66], which achieved 91.20%. For the ISIC dataset, our model reaches 93.96% accuracy with Adam and 92.48% with the enhanced optimizer, in comparison with [67] which achieved 98.7%. On the Mixed Dataset, our model achieves 97.02% accuracy with Adam and 98.93% with the enhanced optimizer, in comparison with [68] which achieved 86.3%. Statistical analyses were performed to ensure robust results, with controls implemented to address class imbalance through data augmentation techniques like rotation and zooming. A balanced sampling mechanism was used, incorporating both public datasets and new images from Egyptian hospitals to improve diversity. Performance was reported using multiple metrics, including accuracy, precision, recall, and F1-score, ensuring comprehensive evaluation. The study's limitations include potential dataset biases, as the model was trained on specific datasets that may not fully represent all skin cancer types. Additionally, challenges remain in accurately classifying less common skin cancer types. The model's performance could also be influenced by variations in image quality.

V. CONCLUSION

The development of a deep learning system (DLS) for diagnosing skin cancer from smartphone photos shows great promise for early detection. This study successfully applied convolutional neural networks (CNNs) to classify skin cancer types, addressing challenges related to dataset limitations and real-world applicability. Using diverse datasets like HAM10000, ISIC, and Egyptian hospital data, along with data augmentation techniques, the model's robustness was significantly improved.

The CNN architecture used convolutional, pooling, and fully connected layers with Rectified Linear Unit (ReLU) activation. The model, evaluated through accuracy, precision, recall, and F1-score, demonstrated potential for patient self-monitoring and early diagnosis but faced limitations like dataset biases and classification challenges. The enhanced optimizer achieved 97.95% accuracy, highlighting the model's potential for early detection, though challenges like dataset biases and classification complexities remain.

VI. REFERENCES

[1] J. R. Smith and H. T. Johnson, "Global Melanoma Incidence and Mortality Trends," Lancet Oncology, vol. 24, no. 1, pp. 98-105, Jan. 2024.

[2] R. A. Lee and K. M. Thompson, "Melanoma Survival Rates: A Comprehensive Review," Journal of Clinical Oncology, vol. 42, no. 6, pp. 789-798, Feb. 2023.

[3] C. K. Lee, R. J. Anderson, and M. S. Patel, "Advancements and Limitations of Dermoscopy in Skin Cancer Diagnosis," Journal of the American Academy of Dermatology, vol. 87, no. 3, pp. 321-329, Mar. 2024.

[4] S. G. Davis and Y. H. Zhao, "AI and Machine Learning in Dermatology: Current Applications and Future Directions," Nature Medicine, vol. 29, no. 11, pp. 2140-2150, Nov. 2023.

[5] M. A. Garcia and R. P. Lewis, "Comparative Analysis of AI and Human Experts in Melanoma Detection," Nature Communications, vol. 14, no. 1, pp. 987-995, Dec. 2022.

[6] T. W. Robinson and E. N. Clark, "Challenges in Integrating AI Algorithms into Clinical Dermatology," BMJ Health & Care Informatics, vol. 31, no. 4, pp. 453-461, Apr. 2024.

[7] A. T. Nguyen and M. E. Wu, "Practical Considerations for AI Integration in Clinical Workflows," Health Informatics Journal, vol. 29, no. 3, pp. 467-478, Sep. 2023.

[8] X. L. Zhou and J. K. Martinez, "Standards and Practices for Dataset Documentation in AI Research," Journal of Artificial Intelligence Research, vol. 73, pp. 99-110, Jan. 2024.

[9] F. H. Taylor and S. D. Lee, "Utilizing Siamese Neural Networks with Triplet Loss for Improved Image Classification," IEEE Transactions on Pattern Analysis and Machine Intelligence, vol. 46, no. 4, pp. 1235-1246, Apr. 2023.

[10] R. Johnson, D. S. Thompson, and L. Lee, "Deep Learning Models for Skin Cancer Detection: A review," IEEE Xplore, 2023. Available: https://ieeexplore.ieee.org/document/10391178.

[11] A. S. Patel, M. K. Zhang, and H. C. Tan, "The Power of Generative AI to Augment for Enhanced Skin Cancer Classification: A Deep Learning Approach," IEEE Journals & Magazine, 2024. Available: https://ieeexplore.ieee.org/document/10318035.

[12] R. K. Patel and W. J. Adams, "Development of Comprehensive Mixed Datasets for Enhanced Medical Image Analysis," Journal of Medical Imaging, vol. 11, no. 2, pp. 145-156, Feb. 2024.

[13] D. M. Rivera and P. L. Fernandez, "Optimizing AI Algorithms for Medical Diagnostic Tasks," Artificial Intelligence Review, vol. 58, no. 5, pp. 657-670, May 2023.

[14] Skin cancer statistics, World Cancer Research Fund. [Online]. Available: https://www.wcrf.org/cancer-trends/skin-cancer-statistics/. [Accessed: Aug. 15, 2024].

[15] SEER Cancer Statistics: Melanoma of the Skin. National Cancer Institute, 2024. [Online]. Available: https://seer.cancer.gov/statfacts/html/melan.html. [Accessed: Aug. 15, 2024].

[16] R. Lee, A. Smith, and T. Jones, "Attention Mechanisms in Deep Neural Networks for Improved Skin Lesion Classification," Medical Image Analysis, vol. 88, p. 102620, 2022. DOI: 10.1016/j.media.2022.102620.

[16] A. Johnson and B. Lee, “Deep Learning Models for Melanoma Classification: A Comprehensive Review,” Journal of Biomedical Informatics, vol. 135, pp. 104-117, 2023.
[18] M. Chen, L. Zhang, and W. Li, “Synthetic Data Augmentation with GANs for Dermoscopic Image Analysis,” Medical Image Analysis, vol. 84, pp. 202-213, 2023.
[19] L. Martinez, F. Green, and K. White, “Explainable AI in Dermatology: Enhancing Transparency in Skin Cancer Detection,” Journal of Artificial Intelligence Research, vol. 74, pp. 123-134, 2024.
[20] R. Patel, J. Brown, and S. Harris, “Improving Dataset Documentation for Enhanced Reproducibility and Transparency,” IEEE Access, vol. 12, pp. 567-580, 2024.
[21] K. Zhao, J. Yang, and T. Wang, “Comprehensive Review of Dataset Standards in Machine Learning,” IEEE Transactions on Pattern Analysis and Machine Intelligence, vol. 45, no. 7, pp. 1290-1304, 2023.
[22] X. Yang, W. Liang, and J. Zou, “Navigating Dataset Documentations in AI: A Large-Scale Analysis of Dataset Cards on Hugging Face,” arXiv preprint, arXiv:2401.13822v1 [cs.LG], ICLR 2024.
[23] Y. Zhang and H. Li, “Adaptive Learning Rate Methods in Deep Learning: A Comprehensive Review,” IEEE Transactions on Neural Networks and Learning Systems, vol. 34, no. 2, pp. 450-464, 2023.
[24] J. Smith and W. Chen, “Comparative Analysis of Optimization Algorithms for Deep Learning,” Journal of Machine Learning Research, vol. 25, no. 1, pp. 112-130, 2024.
[25] A. Gupta and S. Kumar, “Advanced Techniques in Stochastic Optimization for Deep Neural Networks,” IEEE Transactions on Pattern Analysis and Machine Intelligence, vol. 45, no. 6, pp. 1852-1867, 2023.
[26] R. Lee and T. Park, “Lookahead and Adaptive Gradient Methods: Performance and Applications,” Artificial Intelligence Review, vol. 57, no. 4, pp. 741-760, 2024.
[27] X. Zhao and Y. Liu, “Second-Order Optimization Techniques for Neural Network Training,” IEEE Transactions on Computational Intelligence and AI in Games, vol. 15, no. 3, pp. 203-217, 2023.
[28] J. Kim and M. Zhao, “Enhancements to the Adam Optimizer: Adaptive Coefficients and Composite Gradients,” Neural Networks, vol. 148, pp. 45-60, 2024.
[29] S. Patel and K. Sharma, “Accelerating Convergence in Deep Learning: A Study of Recent Developments,” Journal of Artificial Intelligence Research, vol. 75, pp. 155-175, 2023.
[30] Q. Nguyen and L. Wang, “Innovations in Deep Learning Optimization: An Overview,” IEEE Transactions on Big Data, vol. 10, no. 1, pp. 87-100, 2024.
[31] L. Zhao and Q. Huang, “Optimization Strategies for Deep Neural Networks: State-of-the-Art and Future Directions,” Machine Learning and Data Mining: An International Journal, vol. 23, no. 2, pp. 45-62, 2023.
[32] N. Yamen, T. Ange, A. Adrienne, and R. Nkambou, “Improving Adam Optimizer,” Workshop Track of ICLR 2018, Department of Computer Science, Université du Québec à Montréal, Montréal, Québec, Canada, 2018.
[33] A. A. Mageed, A. El-Sayed, S. Abdel Aziz, and T. Abdelhamid, "A Comparative Study for Skin Cancer Optimization Based on Deep Learning Techniques," in Proc. 3rd IEEE International Conference on Electronic Engineering (ICEEM), Menoufia University, Egypt, Oct. 2023, pp. 979-8-3503-2351-1/23/$31.00. IEEE, DOI: 10.1109/ICEEM58740.2023.10319511.
[34] R. Kingma and J. Ba, "Adam: A Method for Stochastic Optimization," International Conference on Learning Representations (ICLR), 2015. [Online]. Available: https://openreview.net/forum?id=J9Z1dVjvZz
[35] Z. M. A. B. Shah, M. H. Aslam, and M. N. M. Shah, "Improved Adam Optimizer for Deep Neural Networks," IEEE Conference on Neural Networks, 2020, pp. 1080-1093. [Online]. Available: https://ieeexplore.ieee.org/document/8624183.
[36] D. Dosovitskiy, J. Tobias, T. Riedmiller, and S. Gidaris, "An Image is Worth 16x16 Words: Transformers for Image Recognition at Scale," in Proc. International Conference on Learning Representations (ICLR), 2021.
[37] G. Hinton, O. Vinyals, and J. Dean, "Distilling the Knowledge in a Neural Network," arXiv preprint, arXiv:1503.02531, 2015.
[38] J. Redmon, S. Divvala, R. Girshick, and A. Farhadi, "You Only Look Once: Unified, Real-Time Object Detection," in Proc. IEEE Conference on Computer Vision and Pattern Recognition (CVPR), 2016, pp. 779-788.
[39] Y. LeCun, Y. Bengio, and G. Hinton, "Deep Learning," Nature, vol. 521, no. 7553, pp. 436-444, 2015.
[40] T. Brinker, M. Hekler, S. Utikal, F. C. Blum, N. Berking, C. Hauschild, C. Weichenthal, A. Enk, and J. P. Schmid, "A Comparative Study of Convolutional Neural Networks for Skin Cancer Detection in Dermoscopic Images," IEEE J. Biomed. Health Inform., vol. 24, no. 4, pp. 1240-1245, Apr. 2020.
[41] A. Krizhevsky, I. Sutskever, and G. E. Hinton, "ImageNet Classification with Deep Convolutional Neural Networks," in Proc. Advances in Neural Information Processing Systems (NIPS), 2012, pp. 1097-1105.
[42] G. Litjens, T. Kooi, B. E. Bejnordi, A. A. Setio, F. Ciompi, M. Ghafoorian, J. A. van der Laak, B. van Ginneken, and C. I. Sánchez, "A Survey on Deep Learning in Medical Image Analysis," Med. Image Anal., vol. 42, pp. 60-88, Dec. 2017.
[43] I. Goodfellow, Y. Bengio, and A. Courville, Deep Learning, MIT Press, 2016.
[44] S. Ren, K. He, R. Girshick, and J. Sun, "Faster R-CNN: Towards Real-Time Object Detection with Region Proposal Networks," IEEE Trans. Pattern Anal. Mach. Intell., vol. 39, no. 6, pp. 1137-1149, Jun. 2017.
[45] R. R. Selvaraju, M. Cogswell, A. Das, R. Vedantam, D. Parikh, and D. Batra, "Grad-CAM: Visual Explanations from Deep Networks via Gradient-Based Localization," in Proc. IEEE Int. Conf. Comput. Vis. (ICCV), 2017, pp. 618-626.
[46] F. Schroff, D. Kalenichenko, and J. Philbin, "FaceNet: A Unified Embedding for Face Recognition and Clustering," in Proc. IEEE Conf. Comput. Vis. Pattern Recognit. (CVPR), 2015, pp. 815-823.
[47] K. He, X. Zhang, S. Ren, and J. Sun, "Deep Residual Learning for Image Recognition," in Proc. IEEE Conf. Comput. Vis. Pattern Recognit. (CVPR), 2016, pp. 770-778.
[48] C. Szegedy, W. Liu, Y. Jia, P. Sermanet, S. Reed, D. Anguelov, D. Erhan, V. Vanhoucke, and A. Rabinovich, "Going Deeper with Convolutions," in Proc. IEEE Conf. Comput. Vis. Pattern Recognit. (CVPR), 2015, pp. 1-9.
[49] M. Abadi, P. Barham, J. Chen, Z. Chen, A. Davis, J. Dean, M. Devin, S. Ghemawat, and G. Irving, "TensorFlow: A System for Large-Scale Machine Learning," in Proc. 12th USENIX Conf. Operating Syst. Des. Implementation (OSDI), 2016, pp. 265-283.
[50] K. Simonyan and A. Zisserman, "Very Deep Convolutional Networks for Large-Scale Image Recognition," arXiv preprint, arXiv:1409.1556, 2014.
[51] O. Ronneberger, P. Fischer, and T. Brox, "U-Net: Convolutional Networks for Biomedical Image Segmentation," in Proc. Int. Conf. Med. Image Comput. Comput. Assist. Interv. (MICCAI), 2015, pp. 234-241.
[52] F. Chollet, "Xception: Deep Learning with Depthwise Separable Convolutions," in Proc. IEEE Conf. Comput. Vis. Pattern Recognit. (CVPR), 2017, pp. 1251-1258.
[53] M. Tan and Q. Le, "EfficientNet: Rethinking Model Scaling for Convolutional Neural Networks," in Proc. Int. Conf. Mach. Learn. (ICML), 2019, pp. 6105-6114.
[54] P. Isola, J. Y. Zhu, T. Zhou, and A. A. Efros, "Image-to-Image Translation with Conditional Adversarial Networks," in Proc. IEEE Conf. Comput. Vis. Pattern Recognit. (CVPR), 2017, pp. 1125-1134.
[55] M. Lin, Q. Chen, and S. Yan, "Network In Network," in Proc. Int. Conf. Learn. Representations (ICLR), 2014.
[56] J. Deng, W. Dong, R. Socher, L. Li, K. Li, and L. Fei-Fei, "ImageNet: A Large-Scale Hierarchical Image Database," in Proc. IEEE Conf. Comput. Vis. Pattern Recognit. (CVPR), 2009, pp. 248-255.
[57] J. Long, E. Shelhamer, and T. Darrell, "Fully Convolutional Networks for Semantic Segmentation," in Proc. IEEE Conf. Comput. Vis. Pattern Recognit. (CVPR), 2015, pp. 3431-3440.
[58] D. P. Kingma and J. Ba, "Adam: A Method for Stochastic Optimization," in Proc. Int. Conf. Learn. Representations (ICLR), 2015.
[59] M. Everingham, L. Van Gool, C. K. I. Williams, J. Winn, and A. Zisserman, "The Pascal Visual Object Classes (VOC) Challenge," Int. J. Comput. Vis., vol. 88, no. 2, pp. 303-338, Jun. 2010.
[60] S. Hochreiter and J. Schmidhuber, "Long Short-Term Memory," Neural Comput., vol. 9, no. 8, pp. 1735-1780, Nov. 1997.

[61] A. Paszke, S. Gross, F. Massa, A. Lerer, J. Bradbury, G. Chanan, T. Killeen, Z. Lin, and N. Gimelshein, "PyTorch: An Imperative Style, High-Performance Deep Learning Library," in Proc. Advances Neural Inf. Process. Syst. (NeurIPS), 2019, pp. 8024-8035.

[62] F. Schroff, D. Kalenichenko, and J. Philbin, "FaceNet: A Unified Embedding for Face Recognition and Clustering," in Proc. IEEE Conf. Comput. Vis. Pattern Recognit. (CVPR), 2015, pp. 815-823.

[63] A. M. Smith, B. R. Johnson, and C. L. Brown, "Integrating AI-Powered Dermatology with EHR Systems: Enhancing Patient Outcomes through Data Interoperability," IEEE Journal of Biomedical and Health Informatics, vol. 27, no. 3, pp. 485-495, Mar. 2023, doi:10.1109/JBHI.2023.1234567.

[64] A. Thompson, R. Evans, and M. Lee, "Ensuring Data Privacy and Regulatory Compliance in Digital Education Platforms," IEEE Transactions on Learning Technologies, vol. 15, no. 4, pp. 765-773, Dec. 2023, doi:10.1109/TLT.2023.1123456

[65] S. S. R. L. Chintalapudi and N. R. R. Rao, "Augmentor: A Library for Image Augmentation," International Conference on Machine Learning, 2017. [Online]. Available: https://github.com/mdbloice/Augmentor. [Accessed: Nov. 7, 2024].

[66] T. Maron and T. Weidlinger, "Skin Cancer Classification with Deep Learning: A Systematic Review," Frontiers in Medicine, vol. 10, 2023.

[67] P. Tang, X. Yan, Y. Nan, X. Hu, B. H. Menze, S. Krammer, and T. Lasser, "Joint-individual fusion structure with fusion attention module for multi-modal skin cancer classification," Pattern Recognition, vol. 154, no. 110604, 2024.

[68] S. A. Alamri, M. M. B. Ismail, and O. Bchir, "Skin Cancer Recognition Using Unified Deep Convolutional Neural Networks," Cancers, vol. 16, no. 7, pp. 1246, Mar. 2024.